Anal. Bioanal. Electrochem., Vol. 17, No. 4, 2025, 256-272
https://www.doi.org/10.22034/abec.2025.723269

Analytical & Bioanalytical Electrochemistry

Full Paper

Development of Tyrosinase-Enhanced Carbon Nanotube Biosensor for Rutin Detection: A Voltametric Approach

P. Gopal,[1,2] G. Narasimha,[3] and T. Madhusudana Reddy[1,*]

[1]*Electrochemical Research Laboratory, Department of Chemistry, S.V.U. College of Sciences, Sri Venkateswara University, Tirupati-517502, Andhra Pradesh, India*
[2]*Institute of Animal Reproduction and Food Research, Polish Academy of Sciences, Tuwima Str. 10, 10-748, Olsztyn, Poland*
[3]*Applied Microbiology Laboratory, Department of Virology, Sri Venkateswara University, Tirupati 517502, Andhra Pradesh, India*

*Corresponding Author, Tel.: +91-877-2289303
E-Mail: tmsreddysvu@gmail.com

Received: 1 February 2025 / Received in revised form: 2 April 2025 / Accepted: 24 April 2025 / Published online: 30 April 2025

Abstract- Rutin (RU) is a naturally occurring polyphenolic flavonoid with significant antioxidant properties found in various plants and natural sources. Due to its natural antioxidant activity, RU strengthens the blood vessels and inhibits harmful cancer cells. The current study involves the development of a highly sensitive electrochemical biosensor for detecting RU by modifying a glassy carbon electrode (GCE) using multi-walled carbon nanotubes (MWCNTs) and immobilization of the tyrosinase enzyme (Ty) via drop-casting onto the GCE surface. The evaluation of biosensor performance was illustrated by cyclic voltammetry (CV), electrochemical impedance spectroscopy (EIS), and Tafel plot studies. The electrochemical redox behavior of RU was thoroughly investigated, and a possible redox mechanism was proposed. The effect of supporting electrolyte phosphate buffer solution pH on RU's electrochemical behavior was studied, and pH 6.0 was identified as the optimal pH for further studies. The kinetic studies revealed that the detection process was adsorption controlled. From the scan rate experiments, the surface coverage concentration (Γ), heterogeneous rate constant (ks), and charge transfer coefficient (α) values were calculated. The biosensor showed impressive analytical performance, with a limit of detection of 4.47×10^{-8} M and a limit of quantification of 1.55×10^{-7} M, as found from the linear regression equation. The practical application of the biosensor was proved through tests for repeatability, reproducibility, and stability, confirming its potential for reliable and robust detection of RU.

Keywords- Rutin; Tyrosinase; Multi-walled carbon nanotubes; Heterogeneous rate constant; Electrochemical impedance spectroscopy; Adsorption-controlled process

1. INTRODUCTION

Flavonoids are polyphenolic compounds widely found in plants, fruits, and vegetables with strong antioxidant properties. The antioxidant activity is mainly through their polyphenol structures, allowing them to scavenge free radicals, lower oxidative stress, and protect cells from injury. They are associated with numerous health benefits, such as anti-inflammatory, cardioprotective, and neuroprotective properties [1-4]. RU is a significant flavonoid that can be obtained naturally from different foods, including citrus fruits, noni, black tea, and apple peels, with buckwheat being its richest source [5–8]. When it's combined with proteins, trypsin, and bromelain, RU can significantly strengthen blood vessels, also, its antioxidant properties help to inhibit the proliferation of harmful cancer cells [9–11]. The physiological effects of RU's anti-inflammatory, anti-tumor, and antibacterial qualities make it a well-known medicinal drug [12]. Given its importance, closely monitoring RU has become increasingly vital. In this regard, the current research aimed to establish a reliable method for meticulous monitoring of RU. Various analytical methods have been developed for RU monitoring, including chromatographic, spectroscopic, and other techniques [13,14], however, these techniques come with many challenges, including complicated sample preparations and device upkeep. Due to their affordability, ease of use, speed, and portability, electroanalytical methods like cyclic voltammetry (CV), differential pulse voltammetry (DPV), and electrochemical impedance spectroscopy (EIS) have drawn considerable interest in overcoming the flaws associated with other analytical instruments [15].

Electroanalytical techniques involve measuring current response against the varying anodic and cathodic potentials and consist of a three-electrode voltammetry cell including a working electrode, counter electrode, and reference electrode. When measuring the peak current response, the working electrode is crucial, however, the sensitive determination could not be made using the standard working electrodes, such as glassy carbon electrodes (GCE), carbon paste electrodes (CPE), or platinum electrodes, due to their surface-fouling nature. Researchers have proposed changing the standard electrode surfaces with various conducting and catalytic materials, such as amino acids, dyes, clays, nanomaterials, and various catalytic and inhibitory enzymes, to solve the drawbacks [16–19].

Nanomaterials are precise materials with numerous applications in many fields of science-related research. Carbon-based nanomaterials have become more significant due to their distinctive features in creating semiconductor devices [20,21]. It's been quite something to see the surge of interest in SnS_2 and MoS_2, those layered metal dichalcogenides seem promising for building electrochemical nanosensors [22-24]. Due to their excellent catalytic activity, electrical nature, and mechanical qualities, multi-walled carbon nanotubes have become particularly essential tools in various industries. Electrochemical researchers have directed their attention to carbon nanostructures for electrode surface modification, and in our current experiment, we used them for surface modification using the drop-casting technique [25,26].

The advancement of electrochemical biosensors has increased their superiority in analytical applications in recent years. Enzymes, peptides, antibodies, and other biological components were used to change the electrode surface of the electrochemical biosensors to enable catalytic activity towards a specific analyte with high selectivity and sensitivity. Ty is an oxidase enzyme found in the tissues of plants and catalyzes the synthesis of melanin and other colors. Monophenol monooxidase, another name for Ty, is the enzyme that catalyzes the conversion of phenol into the equivalent keto group. The Ty enzyme's active site consists of two copper atoms, each coupled with three histidine groups [27–29]. By setting up a link with oxygen to create oxytyrosinase, which then coordinates with catechol to produce o-quinone, the Ty can catalyze the catechol moiety. Scheme 1 shows the precise mechanism of Ty enzyme catalytic activity in the oxidation of the catechol moiety [30,31].

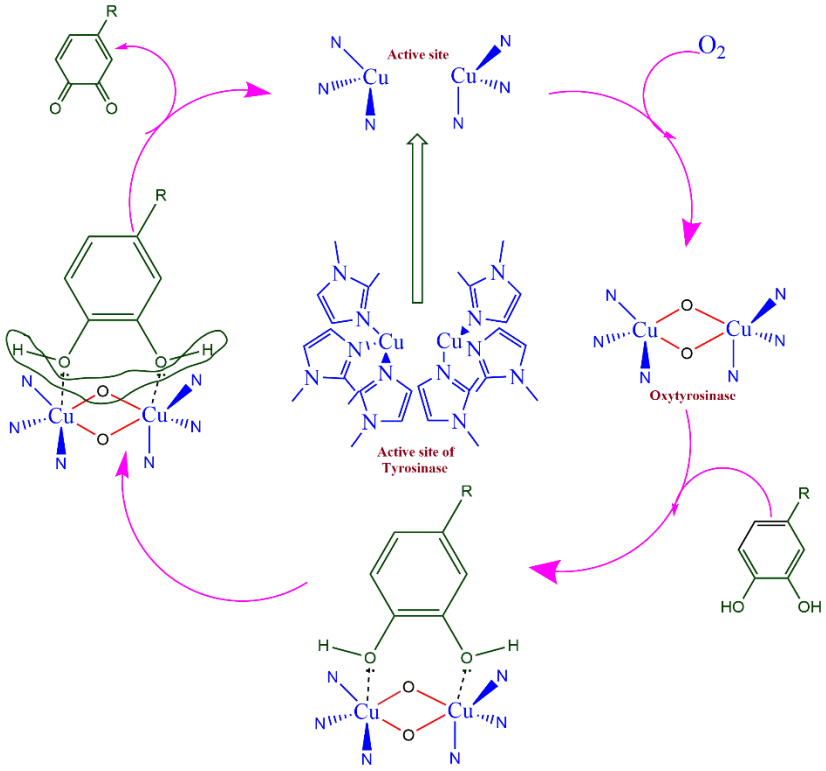

Scheme 1. Schematic illustration of the tyrosinase catalytic reaction mechanism

2. EXPERIMENTAL SECTION

2.1. Materials

All the materials used in the present investigation were received from commercial sources and used without further purification. Rutin (RU) was from Sigma-Aldrich, and multi-walled carbon nanotubes (MWCNT) were from Dropsens, Edificio CEEI, and Llanera (SPAIN). $K_4[Fe(CN)_6]$ and Na_2HPO_4 were from Merck Specialties Pvt. Ltd., Mumbai, and $K_3[Fe(CN)_6]$, NaH_2PO_4 were received from Fisher Scientific India Pvt. Ltd., and the tyrosinase enzyme was obtained from Prof. G. Narasimha, Applied Microbiology Laboratory, Department of

Virology, Sri Venkateswara University, Tirupati, India, which was extracted from Flavadon sps fungi isolated from soil contaminated with industrial waste.

2.2. Methods

The electroanalytical techniques such as cyclic voltammetry, differential pulse voltammetry, and electrochemical impedance spectroscopy were accomplished by using a CH Instruments model CHI 660D, Texas, Austin, with the conventional three-electrode system having a saturated calomel electrode as a reference electrode (provided by CH Instruments (CHI150)), platinum wire (provided by CH Instruments (CHI115)) as a counter electrode and GCE (provided by CH Instruments (CHI104) as a working electrode. Phosphate buffer solutions (PBS) were adjusted to the desired pH values using an ELICO pH meter and glass electrode. The homogeneous suspension of MWCNTs was prepared with a Toshiba ultrasonication bath made in India, and all the measurements were carried out in the Department of Chemistry, Sri Venkateswara University, Tirupati, Andhra Pradesh, India.

2.3. Preparation of MWCNTs suspension and tyrosinase solution

An accurately weighed amount of MWCNTs was dispersed in ethanol to have a homogeneous suspension (1 mg/ 1 mL of MWCNTs) with the help of an ultrasonication bath and stored in the refrigerator at 4℃. The tyrosinase enzyme was accurately weighed and dissolved in PBS at a pH of 6.5 to yield a 1mg/1 mL solution.

2.4. Preparation of Ty/MWCNT/GCE electrode

At first, the bare GCE was polished to a mirror shine with the help of 1 micron, 0.3 micron, and 0.05 micron alumina slurry. After obtaining mirror shine, 5µL of MWCNTs suspension in ethanol was drop-cast onto the surface of GCE by the physical adsorption method, and it was allowed to dry for half an hour to yield MWCNTs/GCE. The MWCNTs/GCE was further modified with 5 µL of tyrosinase enzyme solution prepared by dissolving 1mg/1 mL in pH 6.5 of phosphate buffer solution, and was dropped onto the surface of the MWCNTs/GCE and dried. The electrode obtained was hereafter referred to as Ty/MWCNTs/GCE.

3. RESULTS AND DISCUSSION

3.1. Characterization of different electrodes with cyclic voltammetry

The fabricated biosensor was characterized with 1 mM $[Fe(CN)_6]^{-3/-4}$ in 0.1 M KCl and the CV technique. From Figure 1a, the peak current at bare GCE for $[Fe(CN)_6]^{-3/-4}$ was found to be 1.482×10^{-5} A, 1.507×10^{-5} A at potentials of 0.246 V, and 0.133 V for both anodic and cathodic peaks with a current ratio (i_p^a/i_p^c) of 0.985 and peak to peak separation (ΔE_p) of 113 mV respectively.

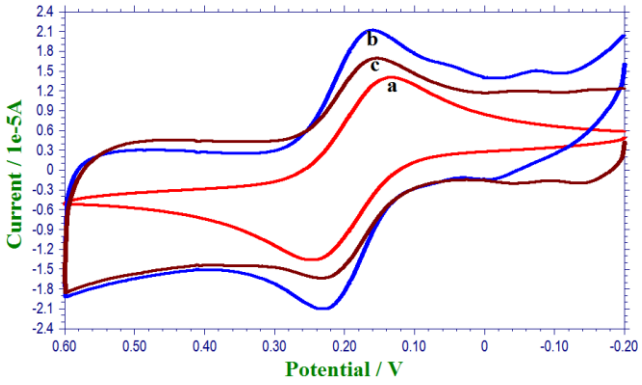

(a)

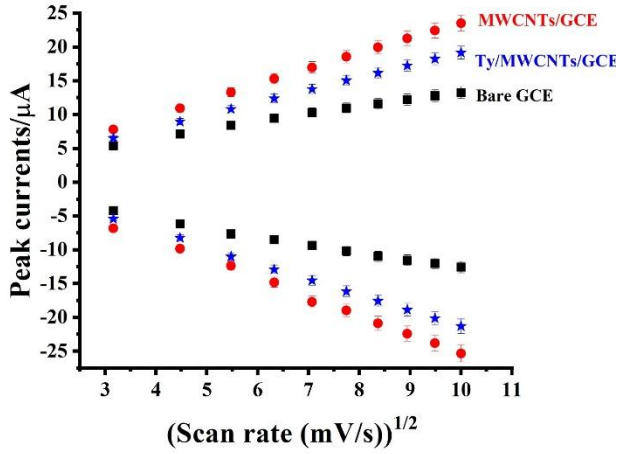

(b)

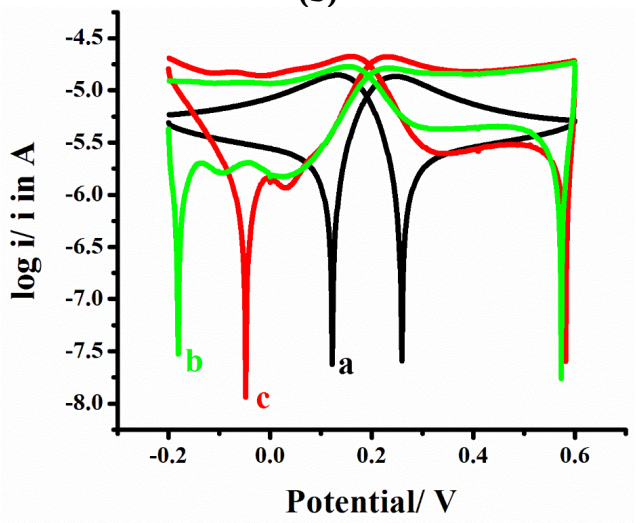

(c)

Figure 1. a) CVs of 1mM $[Fe(CN)_6]^{-3/-4}$ in 0.1 M KCl for bare GCE (a), MWCNTs/GCE (b), and Ty/MWCNTs/GCE (c); **(b)** Plot drawn between the square root of scan rate and peak currents of $[Fe(CN)_6]^{-3/-4}$ at bare GCE (a), MWCNTs/GCE (b), and Ty/MWCNTs/GCE (c); **(c)** A plot is drawn between the logarithm of peak currents from the CV experiment and the corresponding potential of bare GCE (a), MWCNTs/GCE (b), and Ty/MWCNTs/GCE (c)

While the surface of the GCE was modified with MWCNTs, the current response for $[Fe(CN)_6]^{-3/-4}$ was enhanced to 1.986×10^{-5} A, 1.867×10^{-5} A at potentials 0.229 V, 0.160 V for both anodic and cathodic peaks with a current ratio (i_p^a/i_p^c) of 1.064 and peak to peak separation (ΔE_p) of 69 mV respectively.

The increase in the current response and the decrease in the peak-to-peak separation at MWCNTs/GCE were due to the conductive properties of MWCNTs. The redox potentials of $[Fe(CN)_6]^{-3/-4}$ were decreased due to the catalytic nature of MWCNTs, which were adsorbed on the surface of the GCE. Further, the modification of the MWCNTs/GCE surface with tyrosinase enzyme (Ty/MWCNTs/GCE) yielded peak currents of 1.487×10^{-5} A, 1.264×10^{-5} A at potentials of 0.234 V, 0.154 V for $[Fe(CN)_6]^{-3/-4}$ with an anodic and cathodic peak current ratio of (i_p^a/i_p^c) 1.176 and peak to peak separation (ΔE_p) of 80 mV respectively.

From the results, it was seen that the peak currents at Ty/MWCNTs/GCE were decreased, and the peak-to-peak separation was increased, and this may be due to the blocking of catalytic sites of MWCNTs by the tyrosinase enzyme immobilized onto the MWCNTs/GCE. Figure 1b shows the scan rate effect on $[Fe(CN)_6]^{-3/-4}$ at bare GCE, MWCNTs/GCE, and Ty/MWCNTs/GCE. It was found to have good linearity for peak currents versus the square root of scan rate with linear regression equations of i_p^a (µA) = -0. 756 (µA) – 1.207 $\upsilon^{1/2}$ (R^2 = 0.997), i_p^a (µA) = -2.32 (µA) – 2.762 $\upsilon^{1/2}$ (R^2 = 0.998), i_p^a (µA) = -1.946 (µA) – 2.332 $\upsilon^{1/2}$ (R^2 = 0.999), for bare GCE, MWCNTs/GCE and Ty/MWCNTs/GCE respectively. Based on the slopes from the linear regression equations and following the Randles – Sevcik equation (1), we have estimated the active working area for bare GCE, MWCNTs/GCE, and Ty/MWCNTs/GCE as 0.0049 cm^2, 0.0107 cm^2, 0.0081 cm^2 respectively, where i_p^a is the anodic peak currents 'n' is the number of electrons involved in the oxidation process, 'D' is the diffusion coefficient (for $[Fe(CN)_6]^{-3/-4}$ it was used as 7.6×10^{-6} cm^2/s), υ is the scan rate and 'A' is the area of the electrode. From the above-obtained results, it was clear that the modification of bare GCE with MWCNTs facilitated more surface area for the redox reaction of $[Fe(CN)_6]^{-3/-4}$ and further modification with tyrosinase lowers the active surface area by blocking the active sites of MWCNTs [32,33].

$$I_p = 2.69 \times 10^5 n^{3/2} A C D^{1/2} \upsilon^{1/2} \qquad (1)$$

Based on the results obtained from the CV studies, we have plotted a graph between the potential versus the logarithm of currents, and the resulting plot is shown in Figure 1c. From the figure, a small peak separation for the bare GCE was observed for the bare GCE, when the peak separation increased with GCE using MWCNTs, suggesting that the MWCNTs have good catalytic activity and more adsorption properties over the bare GCE surface. Further, the modification of MWCNTs/GCE with tyrosinase enzyme, the peak separation was decreased, suggesting that the immobilized enzyme has no catalytic activity, and the active sites of MWCNTs were blocked by tyrosinase enzyme towards the monitoring of $[Fe(CN)_6]^{-3/-4}$.

3.2. Characterization of electrodes with electrochemical impedance spectroscopy

Electrochemical impedance spectroscopy (EIS) is an advanced analytical method that reveals the surface nature of different materials and is commonly used by many electroanalytical chemists to analyze the surface nature of the modified electrodes. EIS has two types of plots, namely the Bode plot and the Nyquist plot, where the Bode plot is plotted between the logarithm of impedance and phase versus the logarithm of frequency, and the Nyquist plot is plotted between the real and imaginary impedance.

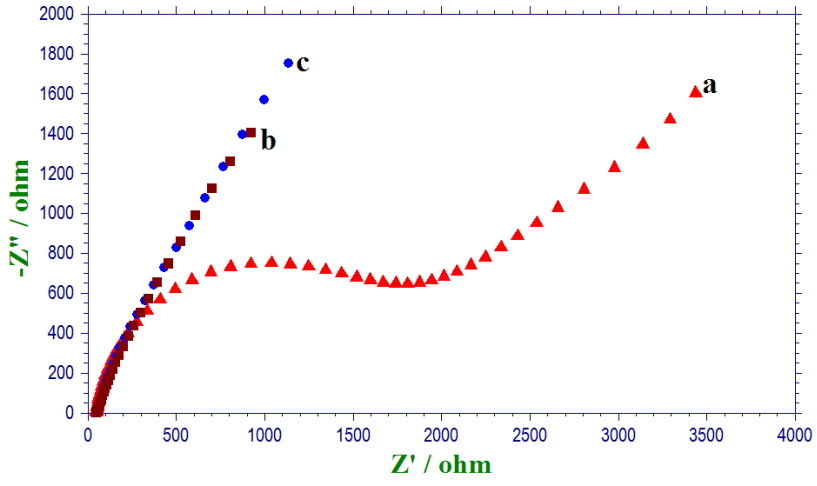

(a)

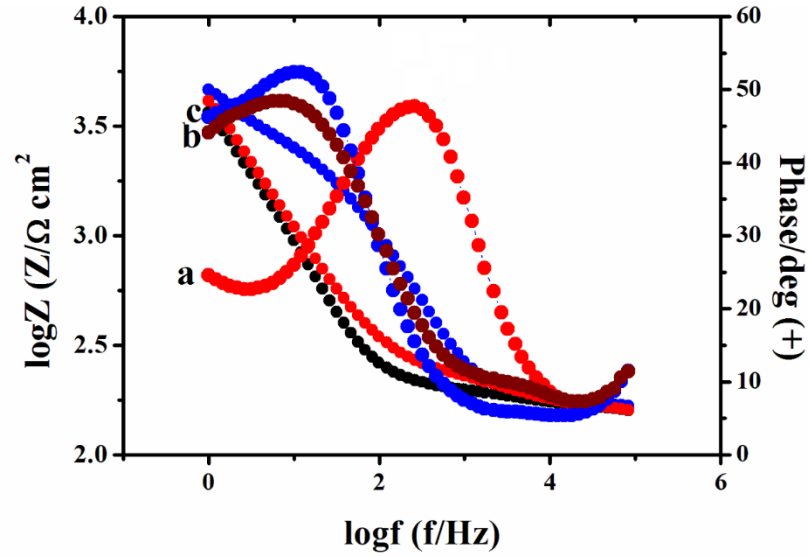

(b)

Figure 2. (a) Nyquist plot for bare GCE (a), MWCNTs/GCE (b), and Ty/MWCNTs/GCE (c); **(b)** The bode plot for bare GCE (a), MWCNTs/GCE (b) and Ty/MWCNTs/GCE (c)

A typical Nyquist plot consists of two portions in which the semicircular part at lower frequencies corresponds to electron transfer resistance (R_{ct}), indicative of kinetic behavior, and

the linear part at lower frequencies stands for the diffusion process. In our present investigation, we have studied EIS for 1 mM $[Fe(CN)_6]^{-3/-4}$ in 0.1 M KCl, and Figure 2a shows the Nyquist plot for bare GCE (a), MWCNTs/GCE (b), and Ty/MWCNTs/GCE (c). The figure shows a large semicircular diameter for bare GCE with a charge transfer resistance of R_{ct} = 1343 Ω. In contrast, the GCE surface modification with MWCNTs led to a significant decrease in the semicircular diameter with a charge transfer resistance of R_{ct} = 14 Ω.

However, a slight increase in the charge transfer resistance to R_{ct} = 20 Ω was observed with the immobilization of tyrosinase onto the MWCNTs/GCE. From the results, the R_{ct} value was decreased from bare GCE to MWCNTs/GCE and increased from MWCNTs/GCE to Ty/MWCNTs/GCE, suggesting that the MWCNTs have more conductive nature and the immobilized tyrosinase lead to an increase in the R_{ct} value, which was due to the blocking of active sites in MWCNTs. Using equation (2), we have evaluated the surface coverage (θ) of Ty/MWCNTs/GCE as 98.51 %. The solution resistance, charge transfer resistance, double layer capacitance, and Warburg impedance data are shown in Table 1. From the table, we have evidence that the double-layer capacitance was increased on modification with MWCNTs and decreased on further modification with Ty. The Warburg impedance results indicate that slower diffusion of the analyte at bare GCE, after the modification with MWCNTs, it led to an increase in the diffusion, and after immobilization of Ty enzyme, the diffusion was slightly decreased and this was due to the lack of attraction between $[Fe(CN)_6]^{-3/-4}$ and electrode surface [34-36].

$$1 - \theta = R_{ct}^{bare} / R_{ct}^{Ty/MWCNTs/GCE} \qquad (2)$$

Table 1. Electrochemical impedance spectroscopy result comparison

Electrode	R_{sol}/Ω	C/μF	R_{ct}/Ω	W
Bare GCE	49.96	0.559	1343	0.000147
MWCNTs/GCE	51.23	24.06	14	0.00022
Ty/MWCNTs/GCE	49.59	20.02	20	0.000167

3.3 Electrochemical redox behavior of Rutin at different electrodes

To understand the electrochemical redox behavior of RU, we have investigated the cyclic voltametric response of 0.1 mM RU in PBS having pH 6.5 with a scan rate of 0.1 V/s at three different electrodes. From Figure 3a, the CV response of RU at bare GCE (a) was less, and on modification of the electrode surface with MWCNTs, the peak currents were increased. This increase in the peak current response was mainly due to the conductive nature of MWCNTs on the electrode surface of GCE. Further, the modifications of MWCNTs/GCE by Ty led to further enhancement in the peak current response, which was due to the catalytic activity of the Ty

enzyme. Based on the results from the CV data and the earlier literature, we have proposed a possible electrochemical redox mechanism of RU at Ty/MWCNTs/GCE. The oxidation of RU at a potential of 0.234 V was due to the conversion of the catechol group into the corresponding o-quinone group [37-39].

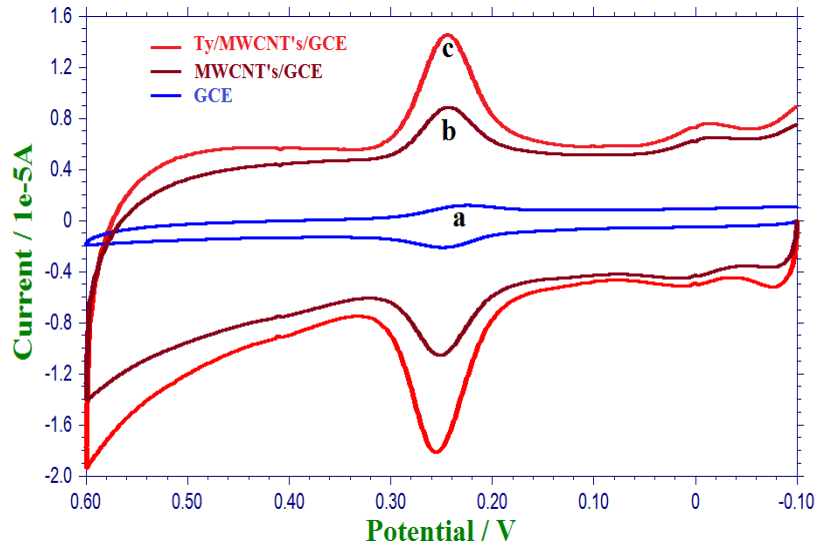

(a)

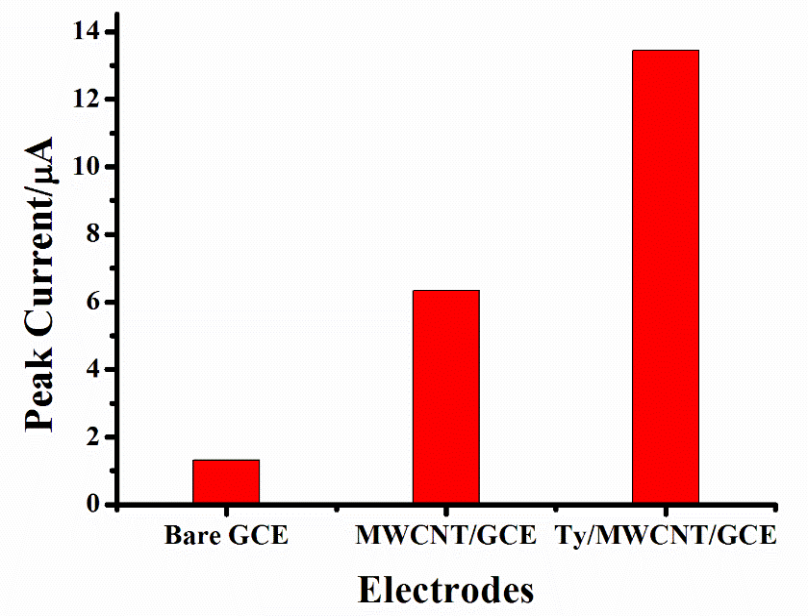

(b)

Figure 3. (a) CVs of 0.1 mM of RU in PBS have pH 6.5 at bare GCE (a), MWCNTs/GCE (b), and Ty/MWCNTs/GCE (c); **(b)** The bar diagram for peak currents at bare GCE, MWCNTs/GCE, and Ty/MWCNTs/GCE

Figure 3b is the graphical representation of the current response at bare GCE, MWCNTs/GCE, and Ty/MWCNTs/GCE, and the electrochemical redox mechanism is emphasized in Scheme 2.

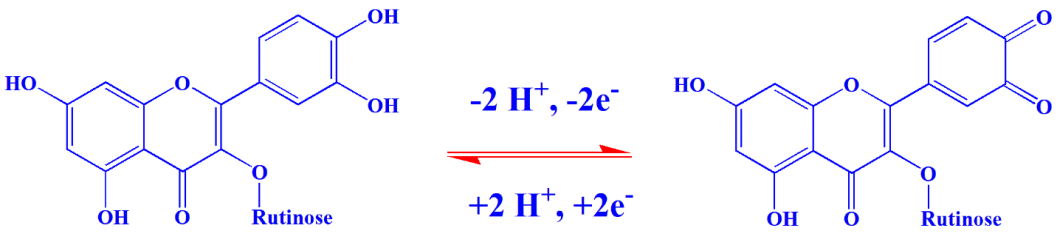

Scheme 2. Proposed electrochemical redox mechanism of RU at Ty/MWCNTs/GCE

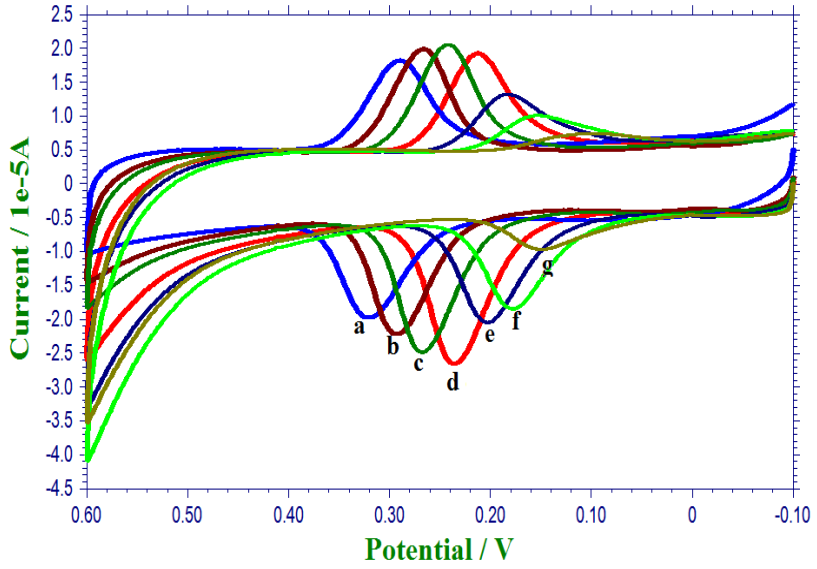

(a)

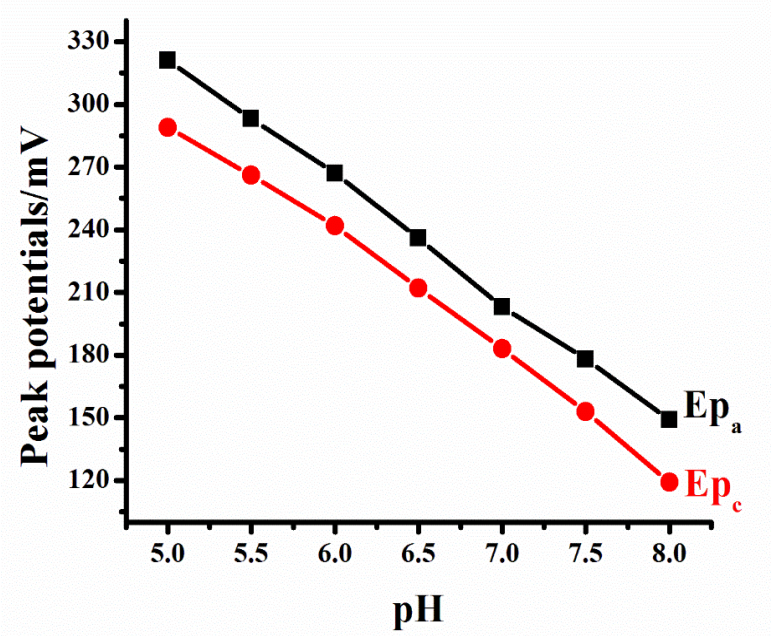

(b)

Figure 4. (a) The CV response of 0.1 mM of RU in PBS having pH 5.0 (a), pH 5.5 (b), pH 6.0 (c), pH 6.5 (d), pH 7.0 (e), pH 7.5 (f), pH 8.0 (g), at Ty/MWCNTs/GCE with scan rate 0.1 V/s; **(b)** A plot is drawn between the peak potential with the corresponding pH

3.4. Effect of pH

To achieve sensitive results for the electrochemical redox behavior of RU, it is essential to study the supporting electrolyte pH on RU at different pH values of PBS at the fabricated electrochemical biosensor. For this purpose, we have examined the CV response of 0.1 mM of RU at different pH mediums of PBS from pH 5.0 to 8.0. It can be seen from Figure. 4a, that the peak potentials were shifted towards low potentials with an increase in the pH of the buffer solution, suggesting the involvement of protons in the electrochemical redox mechanism of RU.

The peak current response of RU was increased by increasing the pH value of PBS, the largest peak currents were noticed at pH 6.5. With a further increase in pH, the peak currents started to decrease, and this increase and decrease in the peak currents are attributed to the fact that the availability of protons is higher in an acidic medium, however, in a basic medium, the peak current decreases due to the lack of availability of protons. The anodic and cathodic peak current ratio was also increased with an increase in the pH values, suggesting that the acidic medium is more favorable for the reversible behavior of RU, and the reversible nature was decreased with an increase in the pH value of PBS. However, we have observed a maximum current response at pH 6.5, which was selected as the optimum pH value for further analysis. From Figure 4b, we have observed a good linearity between the pH of the supporting electrolyte and its corresponding anodic and cathodic peak potentials. The linear regression equation was found to be as E_p^a (mV) = 611.36 (mV) – 57.86 mV/pH, E_p^c (mV) = 578.35 (mV) + 56.79 mV/pH, with correlation coefficient values (R^2) as 0.9995 and 0.9981, respectively. The slope of the linear regression equations was 57.86 mV/pH and 56.79 mV/pH, which were closer to the theoretical slope value of 59 mV/pH, suggesting the Nernst behavior of RU at the developed biosensor with the involvement of an equal number of protons and electrons [40].

3.5. Effect of scan rate

The kinetic behavior and evolution of its parameters are important aspects in the study of the electrochemical behavior of RU. To evaluate the kinetic parameters, we have observed the effect of scan rate on the CV response of 0.1 mM RU with different scan rates ranging from 10 mV to 200 mV. Figure 5a is the CV responses of RU at altered scan rates, the peak current response was gradually increased with an increase in the scan rates. From Figure 5b ‘A’, good linearity was achieved for a log of peak currents against the log of scan rate with the linear equation of log i_p^a = 1.408 + 1.097 log (scan rate) and log i_p^c = 1.411 + 1.149 log (scan rate). The obtained slope values, 1.097 and 1.149, are close to the theoretical value of 1, suggesting the typical adsorption behavior of RU towards the surface of Ty/MWCNTs/GCE. From the CV results, good linearity was achieved for the plot (Figure 5b ‘B’) between the scan rate versus respective anodic and cathodic peak currents with linear regression equation as i_p^a (10^{-5}A) =

0.091 – 21.998 (scan rate) and i_p^a (10^{-5}A) = 0.175 – 20.763 (scan rate) and correlation coefficient (R^2) values of 0.999 and 0.9996 for i_p^a and i_p^c respectively.

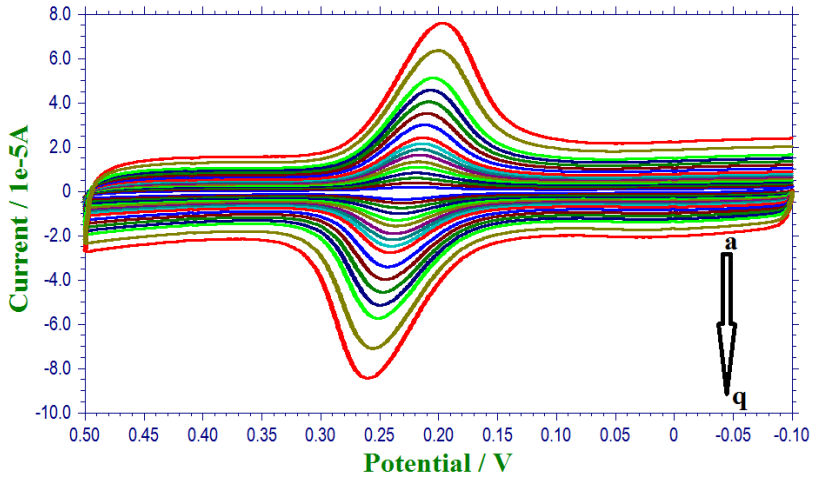

(a)

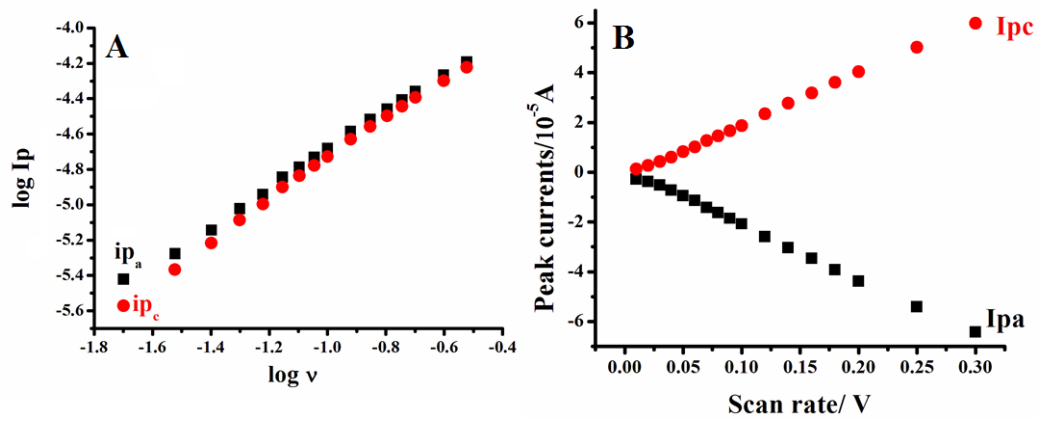

(b)

Figure 5. (a) The CV responses of 0.1 mM of RU at Ty/MWCNTs/GCE in PBS having pH 6.5 with the scan rates of 0.01 V/s (a), 0.02 V/s (b), 0.03 V/s (c), 0.04 V/s (d), 0.05 V/s (e), 0.06 V/s (f), 0.07 V/s (g), 0.08 V/s (h),0.09 V/s (i),0.1 V/s (j), 0.12 V/s (k), 0.14 V/s (l), 0.16 V/s (m), 0.18 V/s (n), 0.2 V/s (o), 0.25 (p), 0.3 (q); **(b)** 'A' is a plot for the logarithm of scan rate versus the logarithm of peak currents. 'B' is a plot drawn between the scan rate and its anodic and cathodic peak currents of RU

A linear plot between scan rate and peak currents suggests that the electrochemical redox behavior of RU was controlled by the adsorption process at Ty/MWCNTs/GCE. By knowing the slope value from the above linearity and substituting it in equation (3), the concentration of the analyte adsorbed onto the surface of Ty/MWCNTs/GCE was calculated, and it was found to be 2.299×10^{-9} mol.cm^{-2}. Further, by using equation (4), the number of electrons involved in

the reaction, charge transfer coefficient (α), and heterogeneous rate constant values were illustrated as 2 electrons, 0.405, and 0.0761 $s^{-1,}$ respectively [41-43].

$$i_p = n^2F^2\upsilon A\Gamma/4RT \qquad (3)$$

$$\log k_s = \alpha \log (1 - \alpha) + (1 - \alpha) \log \alpha - \log (RT/nF\upsilon) - (1 - \alpha)\alpha F\Delta E_p/2.3RT \qquad (4)$$

3.6. Effect of concentration and kinetic investigation

The sensitive nature of the developed electrochemical Ty/MWCNTs/GCE biosensor for RU detection was studied with the help of DPV at optimum conditions. Figure 6a shows the current response of RU at different concentrations, and the peak currents were gradually increasing with an increase in the concentration of RU.

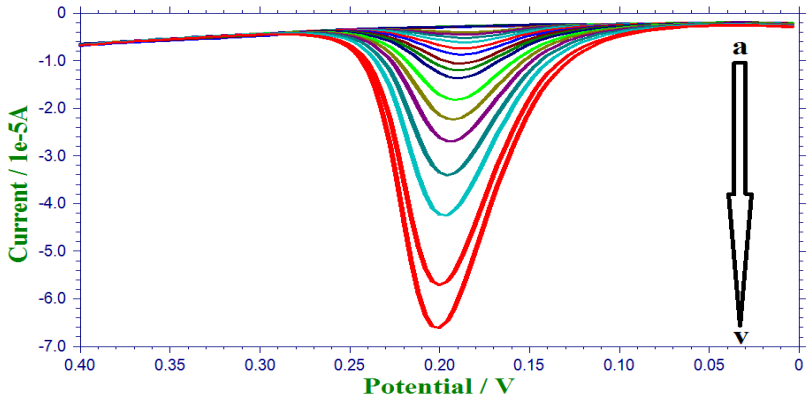

(a)

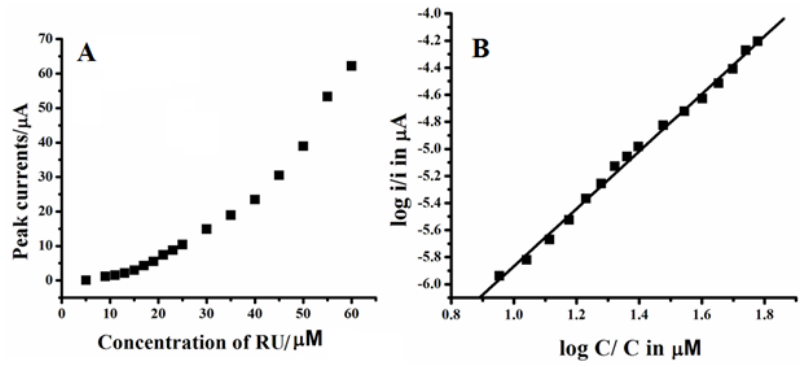

(b)

Figure 6. a) Denotes the DPV's of RU at Ty/MWCNTs/GCE in PBS having pH 6.5 with the concentrations of 5×10^{-6} M (a), 7×10^{-6} M (a), 9×10^{-6} M (b), 11×10^{-6} M (c), 13×10^{-6} M (d), 15×10^{-6} M (e), 17×10^{-6} M (f), 19×10^{-6} M (g), 21×10^{-6} M (h), 23×10^{-6} M (i), 25×10^{-6} M (j), 30×10^{-6} M (k), 35×10^{-6} M (l), 40×10^{-6} M (m), 45×10^{-6} M (o), 50×10^{-6} M (p), 55×10^{-6} M (q), 60×10^{-6} M (r); **(b)** 'A' is the plot located between the concentrations on the X-axis versus peak currents on the Y-axis, and 'B' occupied between the logarithms of concentration versus logarithms of currents

From Figure 6b (A), an anomaly in the relationship between the concentration and respective peak currents is witnessed, and this was due to the absorptive nature of RU on the biosensor's surface, which acts as a self-catalyst. However, good linearity was achieved for the double logarithm of peak currents and concentrations as log i_p^a = 2.009 + 2.136 log (concentration) with a correlation coefficient value of R^2 = 0.9983 [44, 45]. From the above linearity, the slope value was found to be 2.136, which was closer to 2, and from this obtained value, we have concluded that the electrochemical oxidation of RU at Ty/MWCNT/GCE follows second-order kinetics [43]. By using equations (5) and (6) we have calculated the limit of detection (LOD) and limit of quantification (LOQ) as 4.473×10^{-8} M and 1.55×10^{-7} M respectively, where 's' is the standard deviation and 'm' is the slope of the working curve.

$$LOD = 3S/m \qquad (5)$$

$$LOQ = 10S/m \qquad (6)$$

3.7. Repeatability, reproducibility, and stability

Repeatability, reproducibility, and stability are important parameters assessing the practical convenience of the developed Ty/MWCNTs/GCE biosensor. For this reason, we have studied the repeatable nature of the developed biosensor in the presence of 0.1 mM RU with the aid of the CV technique. We recorded different CV responses for the same solution, and the results obtained had almost similar peak current responses with an RSD value of 2.69% for the developed biosensor, suggesting the good repeatable nature of the Ty/MWCNTs/GCE biosensor. Further, to study the reproducible nature of the biosensor, we have measured the current response by CV studies for 0.1 mM RU at different fabricated (Ty/MWCNTs/GCE) electrodes by following the same procedure. The consistent current responses for different biosensors with an RSD value of 4.13% suggest good reproducibility of Ty/MWCNTs/GCE biosensors. We have also studied the stability of the biosensor by seeing the CV responses of 0.1 mM RU in different time intervals, and the results showed very slight variation in the current response with a low RSD value of 5.18%, suggesting the better stability of the developed biosensor. Finally, the repeatability, reproducibility, and stability studies proved that the developed biosensor can be successfully used for analytical purposes [42].

4. CONCLUSION

Herein, we have developed a sensitive method for monitoring RU at the Ty/MWCNTs/GCE biosensor. The biosensor's fabrication involved the drop-casting of GCE with MWCNTs, followed by the subsequent immobilization of the tyrosinase enzyme. The fabricated biosensor was characterized by cyclic voltammetry and impedance spectroscopic studies. The electrochemical redox behavior of RU was examined, and its redox mechanism was proposed. The redox behavior of RU in different pHs of the supporting electrolyte was

studied, and pH 6.5 was selected as an optimum pH value. Further to evaluate the kinetic behavior of RU at the developed biosensor, the effect of scan rate was studied. From the results, we have concluded that the adsorption process controlled the redox behavior of RU at the biosensor. The kinetic parameters, such as charge transfer coefficient, heterogeneous rate constants, and the surface coverage area of RU on the developed biosensor, were also estimated. To determine the sensitivity of the biosensor towards the determination of RU, we have observed the effect of concentration, the limit of detection, and the limit of quantification. The electrochemical oxidation of RU at Ty/MWCNT/GCE followed second-order kinetics. Finally, the biosensor was tested for its repeatability, reproducibility, and stability, and was found in superior condition.

Acknowledgments

One of the authors, P. Gopal, is grateful to the University Grants Commission (UGC), New Delhi, India, for providing financial assistance through a basic scientific research fellowship for meritorious students (BSR-RFMS).

Declarations of interest

The authors declare no conflict of interest in this reported work.

REFERENCES

[1] Z. Manzoor, A. Sajad, S. S. N.Qadiri, et al. Aquacult. Int. 33 (2025) 106.
[2] S. Davidova, A.S. Galabov, and G. Satchanska, Microorganisms 12 (2024) 2502.
[3] A. Gasmi, P.K. Mujawdiya, S. Noor, R. Lysiuk, R. Darmohray, S. Piscopo, L. Lenchyk, H. Antonyak, K. Dehtiarova, M. Shanaida, A. Polishchuk, V. Shanaida, M. Peana, and G. Bjørklund, Molecules 27 (2022) 6280.
[4] Y.M. Reddy, S.P.J. Kumar, K.V. Saritha, P. Gopal, and T.M. Reddy, Plants 10 (2021) 545.
[5] N. Jia, F. Zhang, Q. Liu, L. Wang, S. Lin, and D. Liu, Food Chem. 301 (2019) 125206.
[6] A.M. Chiorcea-Paquim, T.A. Enache, E. Souza Gil, and A.M. Oliveira-Brett, Compr. Rev. Food Sci. Food Saf. 19 (2020) 1680.
[7] K. Yang, F. Han, Y. Jin, and X. Li, Food Chem. 460 (2024) 140382.
[8] T. Zhong, Q. Guo, Z. Yin, X. Zhu, R. Liu, A. Liu, and S. Huang, RSC Adv. 9 (2019) 2152.
[9] K.M. Soto, I. Luzardo-Ocampo, J.M. López-Romero, S. Mendoza, G. Loarca-Piña, E.M. Rivera-Muñoz, and A. Manzano-Ramírez, Pharmaceutics 14 (2022) 2069.
[10] M. Huo, A. Xia, W. Cheng, M. Zhou, J. Wang, T. Shi, C. Cai, W. Jin, M. Zhou, Y. Liao, Z. Liao, Molecules 27 (2022) 2293.

[11] E. Nagles, and O. García-Beltrán, Food Anal. Methods 9 (2016) 3420.
[12] J.G. Manjunatha, B. Kanthappa, N. Hareesha, et al. Chemistry Africa 7 (2024) 1141.
[13] M. Chen, X. Zhang, H. Wang, B. Lin, S. Wang, and G. Hu, J. Chromatogr. Sci. 53 (2015) 519.
[14] S. Hu, H. Zhu, S. Liu, J. Xiang, W. Sun, and L. Zhang, Microchim. Acta 178 (2012) 211.
[15] P. Gopal, G. Narasimha, and T.M. Reddy, Process Biochem. 92 (2020) 476.
[16] P.V. Narayana, T.M. Reddy, P. Gopal, and G.R. Naidu, Anal. Methods 6 (2014) 9459.
[17] P. Gopal, and T.M. Reddy, Colloids Surf. A 538 (2018) 600.
[18] Y. Cui, IEEE Trans. Electron. Devices 64 (2017) 2467.
[19] P. Raghu, T.M. Reddy, K. Reddaiah, B.E.K. Swamy, and M. Sreedhar, Food Chem. 142 (2014) 1886.
[20] T.V. Gopal, T.M. Reddy, and B. Rizwan, J. Environ. Chem. Eng. 12 (2024) 113410.
[21] C. Nesrin, P. Ilknur, B.Y. Bhar, A. Necip, and L.Y. Mehmet, Microchim. Acta 2023, 190, 262.
[22] L.Y. Mehmet, A. Necip, and O. Nermin, Nanoscale 13 (2021) 4660.
[23] S.B. Omer, B.Y. Bahar, B. Havva, and L.Y. Mehmet, Food Chem. Toxicol. 163 (2022) 112994.
[24] T.C. Canevari, M. Nakamura, F.H. Cincotto, F.M. de Melo, and H.E. Toma, Electrochim. Acta 209 (2016) 464.
[25] E. Han, Y. Yang, Z. He, J. Cai, X. Zhang, and X. Dong, Anal. Biochem. 486 (2015) 102.
[26] J. Tang, L. Peng, A. Ali, S. Zhao, Z. Zeng, K. Yuan, and S. Yao, Food Control 155 (2024) 110045.
[27] P. Gopal, T.M. Reddy, and V.N. Palakollu, ChemistrySelect 2 (2017) 3804.
[28] A.V. Bounegru, and C. Apetrei, Enzyme Res. (2014) 163242.
[29] W.T. Ismaya, H. J. Rozeboom, A. Weijn, J.J. Mes, F. Fusetti, H.J. Wichers, and B.W. Dijkstra, Biochemistry 50 (2011) 5477.
[30] G.J. Mattos, C.A.R. Salamanca-Neto, E.C.M. Barbosa, P.H.C. Camargo, R.F.H. Dekker, A.M. Barbosa-Dekker, and E.R.A Sartori, Microchim. Acta 188 (2021) 28.
[31] S. Yang, L. Qu, G. Li, R. Yang, and C. Liu, J. Electroanal. Chem. 645 (2010) 115.
[32] X. Liu, L. Li, X. Zhao, and X. Lu, Colloids Surf. B 81 (2010) 344.
[33] P. Gopal, T.M. Reddy, C. Nagaraju, and G. Narasimha, RSC Adv. 4 (2014) 57591.
[34] N.O. Laschuk, E.B. Easton, and O.V. Zenkina, RSC Adv. 11 (2021) 27925.
[35] K. Silambarasan, N.A.V. Kumar, and J. Joseph, Phys. Chem. Chem. Phys. 18 (2016) 7468.
[36] P. Shaikshavali, T.M. Reddy, G. Venkataprasad, and P. Gopal, J. Iran. Chem. Soc. 15 (2018) 1831.
[37] S. Li, B. Yang, J. Wang, D. Bin, C. Wang, K. Zhang, and Y. Du, Anal. Methods 8 (2016) 5435.

[38] J. Xia, Z. Wang, F. Cai, F. Zhang, M. Yang, W. Xiang, S. Bi, and R. Gui, RSC Adv. 5 (2015) 39131.
[39] K. Reddaiah, T.M. Reddy, Y.S. Rao, P. Raghu, and P. Gopal, Mater. Sci. Eng. B 183 (2014) 69.
[40] P. Raghu, T.M. Reddy, P. Gopal, K. Reddaiah, and N.Y. Sreedhar, Enzyme Microb. Technol. 57 (2014) 8.
[41] P. Gopal, T.M. Reddy, K. Reddaiah, P. Raghu, and P.V. Narayana, J. Mol. Liq. 178 (2013) 168.
[42] E. Laviron, J. Electroanal. Chem. Interfacial Electrochem. 52 (1974) 355.
[43] Z. Liu, Q. Xue, and Y. Guo, Biosens. Bioelectron. 89 (2017) 444.
[44] K. Liu, J. Wei, and C. Wang, Electrochim. Acta 56 (2011) 5189.
[45] S.N.A. Shah, H. Li, and J.M. Lin, Talanta 153 (2016) 230.
[46] G. Venkataprasad, T.M. Reddy, A.L. Narayana, O.M. Husain, P. Shaikshavali, T.V. Gopal, and P. Gopal, Sens. Actuators A Phys. 293 (2019) 87.